

1991

# A new approach to control design : variable gain plots

Thomas R. Kurfess  
*Carnegie Mellon University*

Mark L. Nagurka

Carnegie Mellon University. Engineering Design Research Center.

Follow this and additional works at: <http://repository.cmu.edu/meche>

---

This Technical Report is brought to you for free and open access by the Carnegie Institute of Technology at Research Showcase @ CMU. It has been accepted for inclusion in Department of Mechanical Engineering by an authorized administrator of Research Showcase @ CMU. For more information, please contact [research-showcase@andrew.cmu.edu](mailto:research-showcase@andrew.cmu.edu).

**NOTICE WARNING CONCERNING COPYRIGHT RESTRICTIONS:**

The copyright law of the United States (title 17, U.S. Code) governs the making of photocopies or other reproductions of copyrighted material. Any copying of this document without permission of its author may be prohibited by law.

**A new Approach to Control Design:  
Variable Gain Plots**

by

**Thomas R. Kurfess, Mark. L. Nagurka**

**EDRC 24-43-91**

# **A New Approach to Control Design: Variable Gain Plots**

**T.R. Kurfess and M.X. Nagurka**  
*Department of Mechanical Engineering*  
**Carnegie Mellon University**  
**Pittsburgh, PA 15213**

**February 1991**

**This report proposes a new graphical representation and perspective on the Evans root locus, a well known controls design technique for stability and performance evaluation. The visualization is based on the adjustment of a proportional control gain in the same fashion that is employed in constructing the root locus. The result is a set of Variable Gain Plots (VGPs) that depict the polar coordinates, i.e., magnitude and angle, of each closed loop system eigenvalue in the complex plane as a function of the gain. The VGPs consist of two graphs: (i) magnitude of system eigenvalues vs. gain, and (ii) argument of system eigenvalues vs. gain.**

**The VGPs impart significant insight for determining the values of gain that render a closed-loop system either stable or unstable. By exposing the correspondence of gain values to specific eigenvalues, the VGPs are useful tools for identifying closed-loop designs meeting performance specifications. An additional advantage of the VGPs is their ability to reveal by inspection information about closed-loop sensitivity to gain variations. Finally, the VGPs are applicable to both single-input, single-output (SISO) and multiple-input, multiple-output (MIMO) closed-loop feedback systems. For both cases, the VGPs present eigenvalue trajectories in an informative and unambiguous manner, and serve as a powerful new design paradigm.**

## Introduction

In a sequence of two landmark papers, W.R. Evans presented a technique for analyzing and graphically portraying the loci of closed-loop system poles (Evans, 1948, 1950). Since the publication of these papers, the Evans root locus technique has become a standard and commonly employed synthesis tool of the control design engineer. The root locus plot has several qualities that make it a valuable classical controls tool; perhaps its most valued assets are the ease with which it may be implemented and the tremendous amount of information and insight that it provides.

For most single-input, single-output (SISO) linear time-invariant systems, sketching the root locus as a function of gain is a simple and well documented task. Most undergraduate controls textbooks present the sketching rules for constructing the root locus plot. By following these rules, the loci of roots - or system eigenvalues - may be graphed in the complex plane as certain parameters are varied. Although the methods are applicable and extend to other (real valued) parameters, the most common parameter investigated is the proportional control gain. This is the parameter studied in this report. Even though the sketch may not be exact, the approximate root locus plot provides a plethora of useful information about system stability and performance. For example, closed-loop stability can be determined, and damping and response speed can be estimated as the gain is varied. However, the plot indicates only the trends of the pole locations for varying values of gain, and, in general, does not present specific gain values associated with pole locations.

This report promotes an alternate graphical representation of the root locus plot that exposes the relationship between the pole locations and the gain without sacrificing any of the information presented in the standard root locus. The representation, based on the same Variable Gain Analysis employed by Evans, is summarized by a pair of Variable Gain Plots (VGPs) that casts the magnitude and angle of the system eigenvalues in the complex plane as an explicit function of gain. By utilizing an eigenvalue polar representation, the VGPs present system performance information such as damping and natural frequency in a clear and concise manner. Additionally, eigenvalue sensitivity can be obtained by examining the slopes of the magnitude and angle plots with changing gain. The VGPs can be constructed for, and are applicable to, both SISO and multiple-input, multiple-output (MIMO) systems.

This report is organized into four sections. The following section is a conceptual framework that motivates the development of a pair of plots, namely the VGPs, that offer several advantageous features and serve as rich synthesis tools. In a subsequent section,

several SISO and MIMO examples that demonstrate the utility of the VGPs for stability, performance and sensitivity analyses are presented. Finally, the results of this report are summarized and future research is identified.

## Conceptualization

This section presents a systematic development of the VGPs, an alternate graphical means for representing system behavior. The conceptualization begins with the Evans root locus plot in the traditional two-dimensional complex plane. It is then complemented by a third axis representing the gain. The resulting three-dimensional plot is conformally mapped into a new space that presents polar coordinate information associated with the complex plane. Two orthogonal views of this new three-dimensional space show the VGPs. They present root locus information in a novel and enhanced manner.

The development of the VGPs from the root locus plot is paralleled by the development of the Bode plots from the Nyquist diagram. As such, a fundamental relationship appears to exist between the Bode plots, the Nyquist diagram, Evans root locus, and the VGPs. A unified framework linking these four controls tools is discussed in the closing section of this report.

This section addresses the SISO case, as covered in "classical controls." The analysis, though, may be extended to the MIMO case, and examples of multivariable VGPs are presented in the subsequent section. For purposes of illustration, a single "theme" example given by the open-loop transfer function,  $g(s)$ ,

$$g(s) = \frac{K(s+3)}{(s+1)(s+2)} \quad (1)$$

is investigated here. This transfer function is embedded in a standard closed-loop negative feedback system shown in Figure (1).

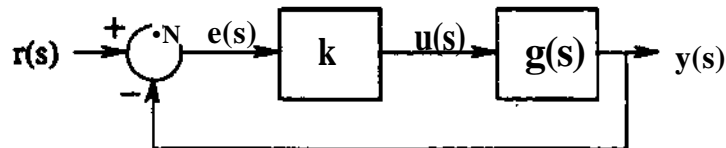


Figure 1. Closed-Loop SISO Negative Feedback Configuration.

## Two Old Friends: Two-Dimensional Polar Representations

### The Nyquist Diagram (Nyquist, 1932)

The Nyquist diagram is a polar plot of a sinusoidal transfer function,  $g(j\omega)$ . The magnitude of  $g(j\omega)$  is plotted against the angle of  $g(j\omega)$  for

$$0 \leq \omega < \infty \quad (2)$$

(The lower limit of equation (2) can alternatively be chosen as  $-\infty$ , with the resulting curve being symmetric about the real axis.) Although the Nyquist diagram is a polar representation, it is graphed in a complex Cartesian plane (two-dimensional space) where the implicit variable is  $\omega$ . Figure 2 is the Nyquist diagram of equation (1) for  $\omega$  given by equation (2). The Nyquist curve starts at  $\omega=0$  corresponding to a D.G gain of 1.5 and phase angle of  $0^\circ$  and asymptotically approaches the origin (zero magnitude) from  $-90^\circ$ .

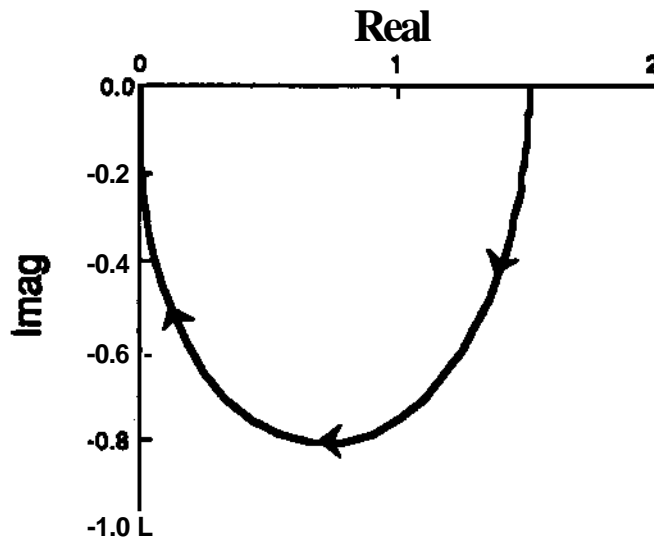


Figure2. The Nyquist Diagram of Equation (1).

It is possible to show the frequency graduation on the locus (with tick marks denoting equal values of  $\omega$ ) or to present superimposed constant frequency contours (Ogata, 1990). However, even if these are added, the Nyquist diagram is not "designed" nor convenient for identifying the frequency associated with a given point on the curve.

### The Evans Root Locus (Evans, 1948,1950)

The root locus plot drawn in the complex plane shows the location of the characteristic roots, *i.e.*, the eigenvalues, in terms of some (real valued) system parameter

such as the proportional gain. It is based on the closed-loop transfer function of Figure 1 given by

$$g_{CL}(s) = \frac{k g(s)}{1 + k g(s)} \quad (3)$$

where  $k$  is the proportional gain. The stability of the closed-loop system is determined by the eigenvalues, which are the solutions of

$$k g(s) = -1 \quad (4)$$

*i.e.*, the denominator roots of equation (3). The root locus is the solution set of equation (4) as the gain  $k$  varies in the range

$$0 \leq k < \infty \quad (5)$$

Equation (4) is equivalent to two conditions: the angle criterion,

$$\angle k g(s) = \pm 180^\circ(2m + 1), \quad m = 0, 1, 2, \dots \quad (6)$$

and the magnitude criterion,

$$|k g(s)| = 1 \quad (7)$$

The shape of the root locus plot is determined entirely by the angle criterion, equation (6). Then, for any eigenvalue  $s$  on the root locus, the magnitude criterion, equation (7), is invoked to solve for the corresponding value of  $k$ . (This process is referred to as scaling the locus.) Figure 3 is the root locus plot of equation (1) for  $k$  given by equation (5). Each branch of the root locus starts at  $k=0$  corresponding to a system open-loop pole, and asymptotically approaches either a finite or infinite transmission zero. It is possible to show the gain graduation on the locus (with tick marks denoting equal values of  $k$ ) or to present superimposed constant gain contours.

The root locus gives a direct indication of closed-loop system instability by observing if branches enter the right half complex plane (indicating positive real-part eigenvalues). Hence, by inspection, it is possible to determine the stability of the closed-loop system as the gain varies. In addition, the root locus plot is a graphical performance tool providing metrics of natural frequency ( $\omega_n$ ) and damping ratio ( $\zeta$ ). These two characteristics, known from magnitude and angle information in the Cartesian plane, enable the calculation of many critical performance indices (damped natural frequency, system time constants, *etc.*) It follows that the root locus plot may be viewed as a polar

magniflnc **and angle** components. An alternative means for expressing the complex value,

$$s = \sigma + j\omega = Re^{j\theta} \quad (8)$$

is to report its angle,  $\theta$ , and magnitude,  $R$ ,

$$\theta = \tan^{-1}(\omega, \sigma) \quad (9)$$

$$R = \sqrt{\sigma^2 + \omega^2} \quad (10)$$

where  $\theta$  in equation (9) is given by the two argument inverse tangent function. Plotting  $\theta$  and  $R$  in a Cartesian plane has significant advantages, as discussed below.

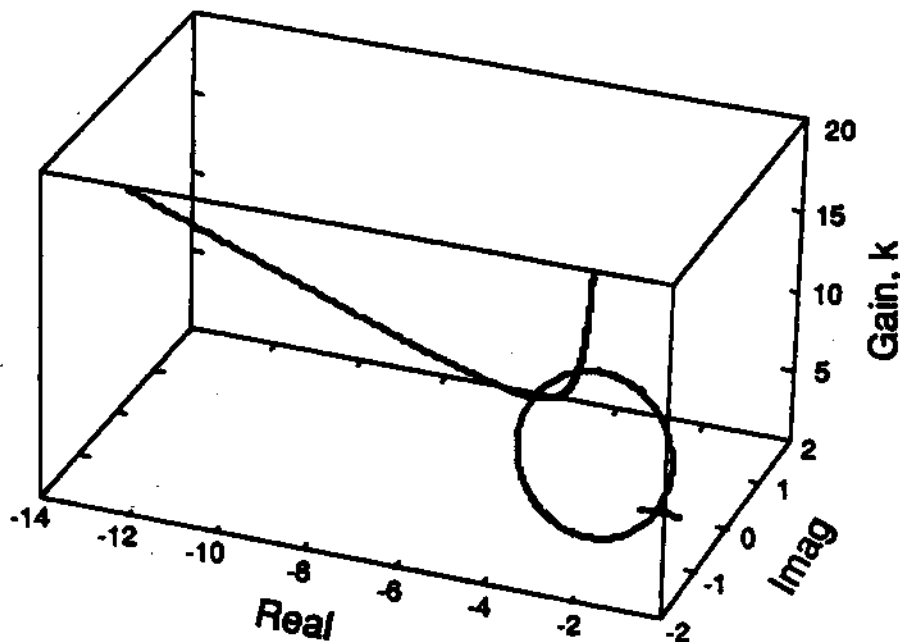


Figure 5. Three Dimensional Evans Root Locus Diagram of Equation (1).

### **Three Dimensional Variable Frequency Plot**

Equations (9) and (10) can be used to transform Figure 4 into Figure 6. This figure shows the effect of frequency on the magnitude and angle of the open-loop system given by equation (1). (For clarification, the curve begins in the front upper left hand corner, and ends at the rear lower right hand corner.) Clearly, this three-dimensional curve is related to well-known variable frequency plots mentioned in the literature (Bode, 1940).

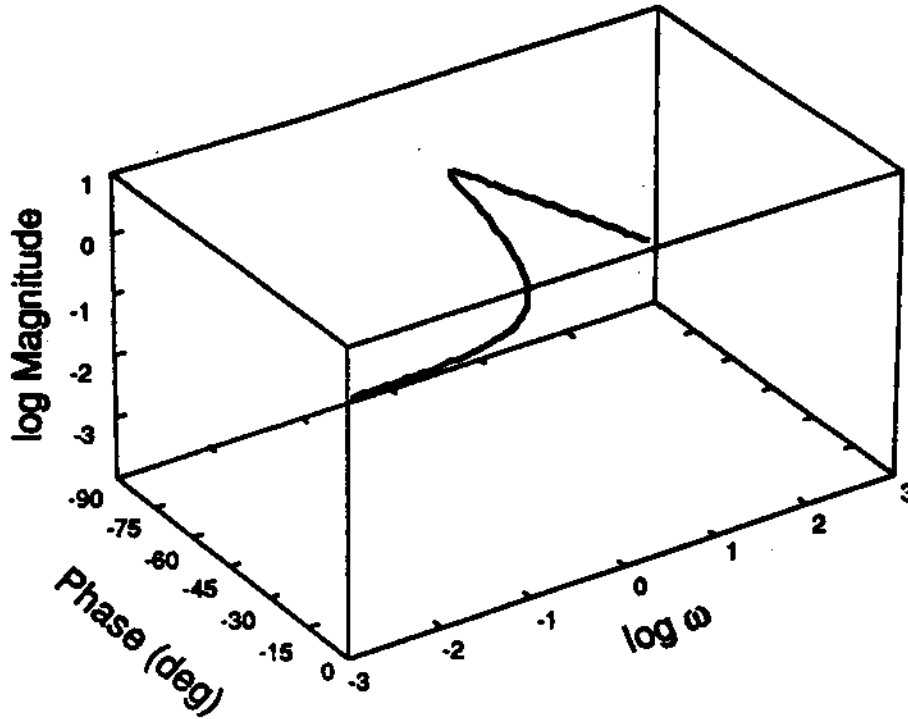


Figure 6. Three Dimensional Variable Frequency Plot of Equation (1).

---

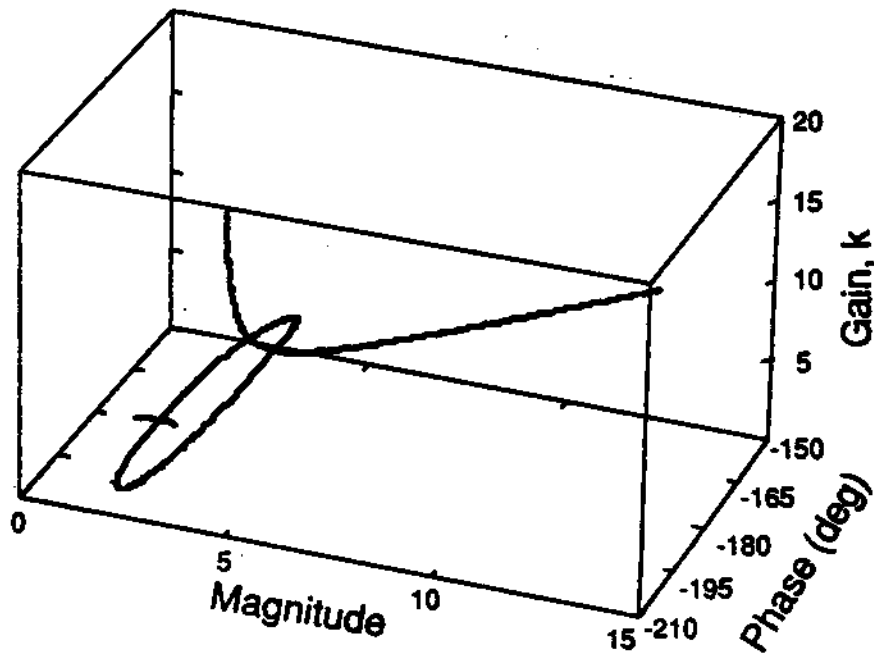


Figure 7. Three Dimensional Variable Gain Plot of Equation (3).

---

### Three Dimensional Variable Frequency Plot (VFP)

Equations (9) and (10) can be used to transform Figure 5 into Figure 7. This figure shows the effect of gain on the magnitude and angle of the closed-loop system given by equation (3). This three-dimensional curve is related to the root-locus diagram.

### An Old and a New Friend: **Two Dimensional Cartesian Representations**

#### The Bode Plots (Bode, 1940)

The Bode plots consist of two planar plots, one called the Bode magnitude plot showing magnitude vs. frequency, and the second called the Bode phase plot reporting phase (angle) vs. frequency. The standard Bode plots employ logarithmic scaling for both the frequency and magnitude axes, and a linear scale for the phase axis. Figures 8a,b are the Bode magnitude and phase plots for the open-loop system given by equation (1).

The Bode plots represent two orthogonal views of the three-dimensional Variable Frequency Plot of Figure 6, *i.e.*, the Bode magnitude plot is seen by observing Figure 6 from a direction orthogonal to the co-magnitude plane and the Bode phase plot is seen by viewing Figure 6 from a direction orthogonal to the co-phase plane. (In fact, Figures 6 and 8 were generated using the same data.) Although the same information is presented in Figures 6 and 8, the traditional Bode plots are significantly simpler to understand. Indeed, Bode plots are among the control designers' most powerful synthesis tools.

#### The Variable Gain Plots (VGPs)

Just as Bode plots simplify the three-dimensional Variable Frequency Plot, VGPs may be employed to simplify the three-dimensional Variable Gain Plot. Figures 9a,b are such a representation for the closed-loop system of equation (3). (Figures 9c,d show a magnified view over the region  $0 \leq k < 0.3$ .) The Variable Gain Magnitude Plot (VGMP) is seen by viewing Figure 7 from a direction orthogonal to the k-magnitude plane and the Variable Gain Angle Plot (VGAP) is seen by observing Figure 7 from a direction orthogonal to the k-phase plane. Although the same information is presented in Figures 7 and 9, the VGPs are significantly simpler to understand.

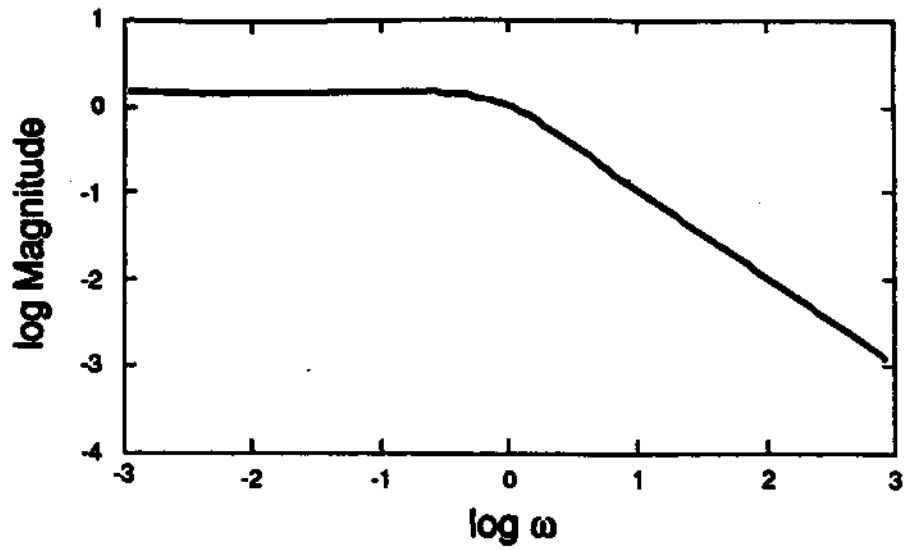


Figure 8a. The **Bode Magnitude Plot** of Equation (1).

---

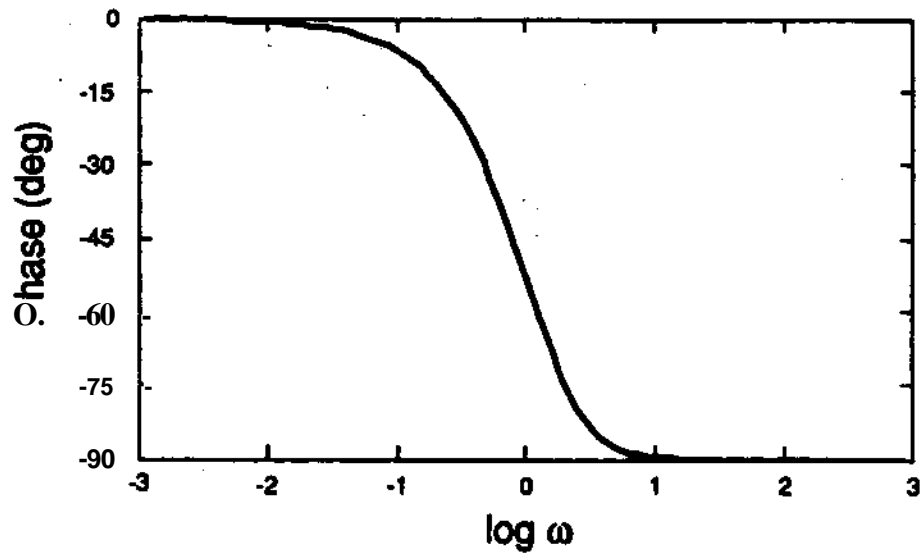


Figure 8b. The Bode Phase Plot of Equation (1).

---

Notice that the eigenvalues are represented by a single line at  $-180^\circ$  on the VGAP when they are real, since they are both on the negative real axis. Conversely, when the eigenvalues are complex conjugates, their magnitudes are equal corresponding to a single segment on the VGMP.

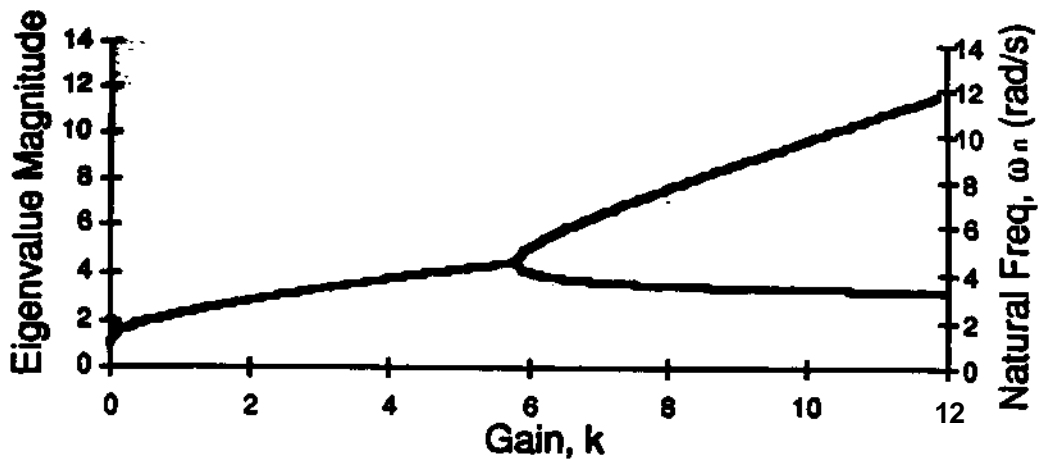


Figure 9a. The Variable Gain Magnitude Plot of Equation (3).

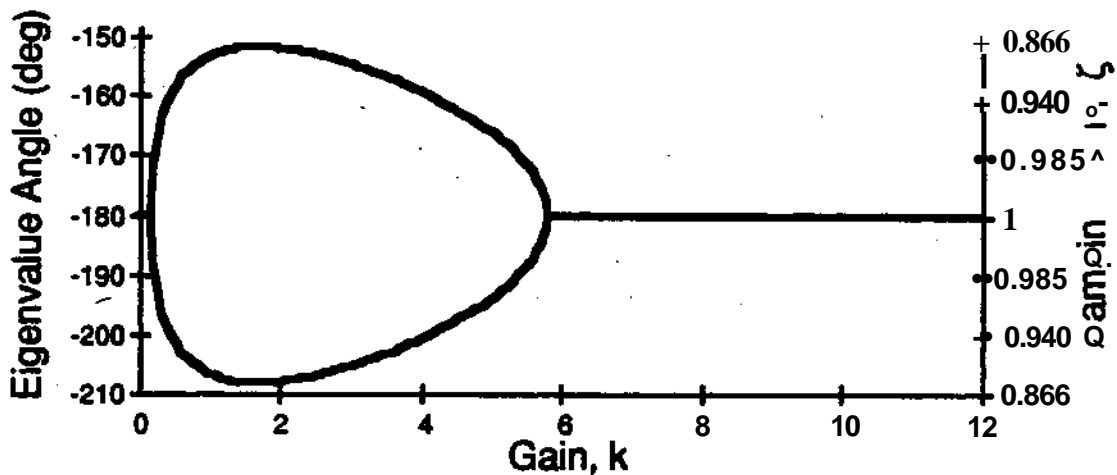
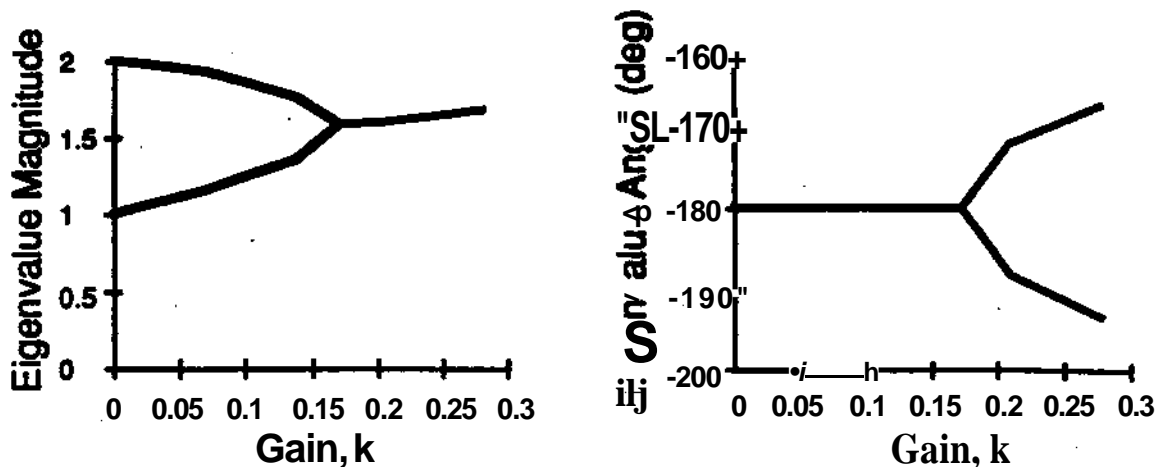


Figure 9b. The Variable Gain Angle Plot of Equation (3).

The VGAP reflects the basic construction rule of the root locus, *i.e.*, the angle criterion of equation (6). As a result, the VGAP is symmetric along the  $-180^\circ$  line. Furthermore, the angle criterion dictates that the eigenvalues must lie on the real axis or be complex conjugates. Thus, a pair of complex conjugate eigenvalues is shown as a single curve in the VGMP with corresponding angles symmetrically configured about the  $-180^\circ$  line shown in the VGAP. As  $k$  varies, the complex conjugate eigenvalues may become distinct real eigenvalues, causing their angles to become equal (at a multiple of  $-180^\circ$ ) and permitting their magnitudes to differ.



Figures 9c,d. Detailed VGPs over the Region  $0 \leq k < 0.3$ .

The VGMP shows the presence of two open-loop poles with magnitudes 1 and 2 at  $k = 0$ . As  $k \rightarrow \infty$  it shows a single finite transmission zero with magnitude 3 and an infinite transmission zero. The VGAP indicates that the two open-loop poles and finite transmission zero are located in the left-half plane since they have angles of  $-180^\circ$ . Furthermore, as  $k \rightarrow \infty$  the VGAP shows that there is an asymptote of  $-180^\circ$  (corresponding to the infinite transmission zero).

Both VGPs highlight the break points corresponding to points where branches leave or enter the real axis of the root locus. For example, these break points occur at  $k \approx 0.17$  and at  $k \approx 5.83$ . Between these break points the VGAP indicates that the loci of the two branch points are not on the real axis and the corresponding single curve of the VGMP confirms that the trajectories are those of a complex conjugate pair.

The VGAP and the VGMP present several important stability and performance features of the system; these are summarized in Figures 10a, b. (In Figure 10b "NA" denotes "Not Applicable.") Stability may be determined from the VGAP by noting if the angle of an eigenvalue meets the following criterion

$$180^\circ(2m+1) - 90^\circ < \angle e < 180^\circ(2m+1) + 90^\circ, \quad m = 0, 1, 2, \dots \quad (11)$$

corresponding to a location in the second and third quadrants of the complex plane. For the case  $m=0$ , equation (11) simplifies to

$$90^\circ < \angle e < 270^\circ \quad (12)$$

The complementary unstable range is shown in the shaded region in Figure 10b.

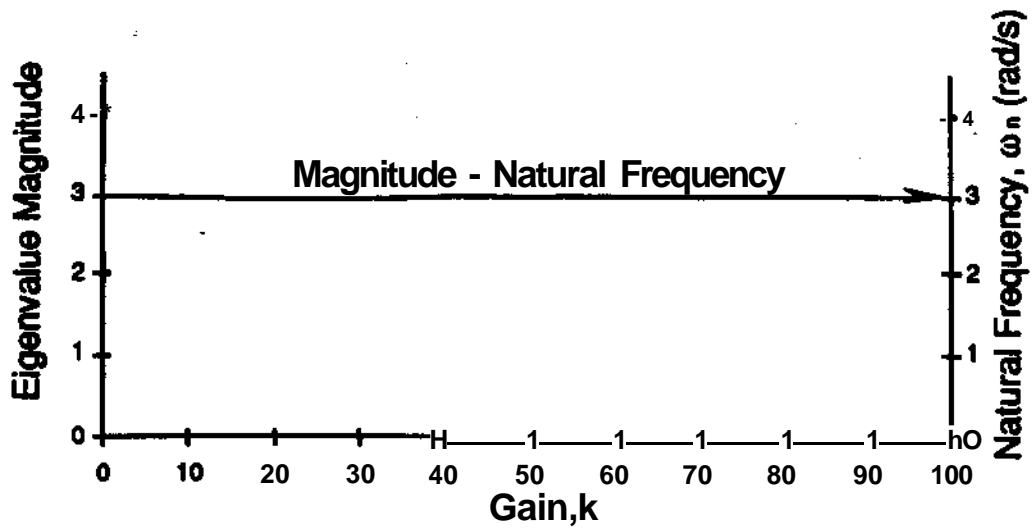


Figure 10a. Parameters in the Variable Gain Magnitude Plot

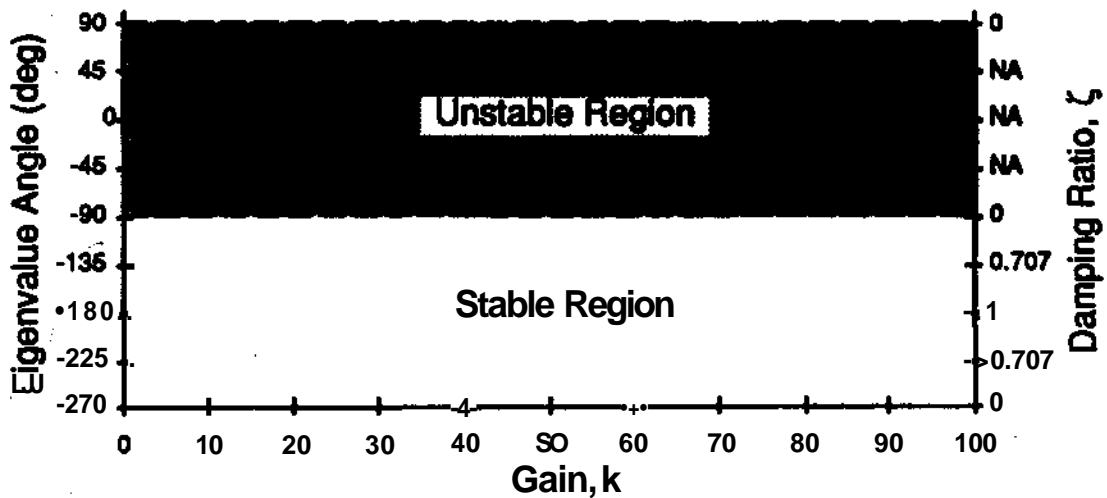


Figure 10b. Parameters in the Variable Gain Angle Plot

The calculations of performance measures are simplified with the VGPs. In particular, the natural frequency,  $\omega_n$  rad/s, is the magnitude shown in the VGMP, and the damping ratio,  $\zeta$ , is

$$C = |\cos-i(e)| \quad (13)$$

where  $e$  is the angle from the VGAP. As shown in Figure 10, supplementary axes can be added to the VGPs to display  $\omega_n$  and  $\zeta$ , directly. If the eigenvalues are on the real axis, the VGMP presents the system time constants.

Although the conventional root locus plot provides such performance information, there are several advantages of the VGPs. First, the value of  $k$  as an independent variable is represented directly on the abscissa. Hence, the influence of gain on ordinate (dependent) variables is exposed explicitly. Second, the performance measures of  $\sigma^*$  and  $\xi$  are represented directly. Thus, given a design specification for  $\sigma^*$  and  $\xi$ , the requisite value of  $k$  may be determined by inspection. A novel feature of the VGPs is this link of performance and gain.

By exposing gain as an independent variable, the VGPs are well suited for determining eigenvalue sensitivity. From the slopes of the VGPs, the sensitivity, *i.e.*, change in magnitude and angle of each eigenvalue per change in gain, can be ascertained. This is useful in the synthesis of control systems that are less sensitive to gain variations.

In addition to the advantages above, the VGPs provide a unified approach for SISO and MIMO systems where compensation dynamics are governed by a single scalar gain amplifying all plant inputs. This is an important advantage since the root locus branches can be identified uniquely as a function of gain. MIMO VGPs are introduced later in two examples.

## Illustrative Examples

This section presents examples that demonstrate the utility of the VGPs. Three examples are presented: (i) a more complicated SISO example, (ii) a decoupled MIMO example, and (iii) a coupled MIMO example.

### Non-Trivial SISO Example

Figure 11 is the root locus plot for the negative feedback system of Figure 1 with the open-loop transfer function

$$g(s) = \frac{(s + 1)}{s(s - 1)(s^2 + 4s + 16)} \quad (14)$$

(Equation (14) is employed in example A-5-3, Ogata, 1990.) The root locus begins at the open-loop poles, *i.e.*, the roots of the denominator of equation (14). These open-loop poles are located at  $s = \{0, +1, -2 \pm \sqrt{7}j\}$ . There is a single finite transmission zero at value  $s = -1$ . The open-loop complex conjugate pole pair migrates to the real axis with increasing gain. One of these poles then proceeds to the finite transmission zero; the other pole moves to an infinite transmission zero along an asymptote of  $-180^\circ$ . The two real open-loop poles migrate to  $s = 0.46$ , and then break out from the real axis. As a complex conjugate

pole pair, they move to the left of the imaginary axis. Subsequently, they migrate back to the right of the imaginary axis and continue toward infinite transmission zeros along asymptotes of  $\pm 60^\circ$ . For a small range of  $k$ , the root locus is located completely within the left half of the complex plane. This range, corresponding to a stable closed-loop system, may be found from the magnitude criterion (equation (7)) to be

$$23.3 < k < 35.7 \quad (15)$$

These gain values are not evident from Figure 11.

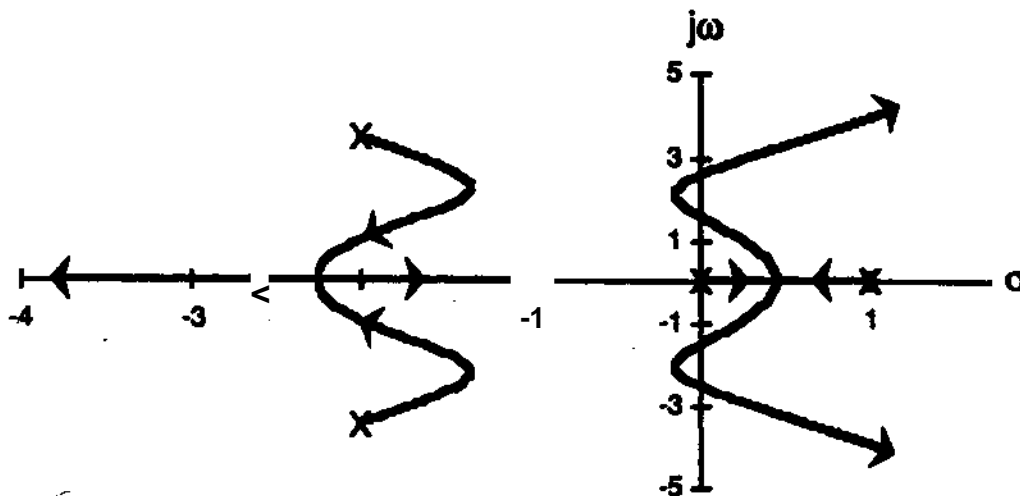


Figure 11. Root Locus for System Given by Equation (14).

Figure 12a,b are the VGPs for the system given by equation (14). Information about the open-loop eigenvalues is shown at  $k = 0$ : (i) there is an unstable set of open-loop poles at an angle of  $0^\circ$  having magnitudes of 0 and 1; and (ii) there is a complex conjugate open-loop pole pair having magnitude 4 at angles of  $-120^\circ$  and  $-240^\circ$ . By inspection, these complex conjugate poles have a natural frequency of 4 rad/s and a damping ratio of 0.5, although this information is "secondary" since the open-loop system is unstable. In Figure 12a,b additional vertical axes reporting natural frequency and damping ratio are shown.

For positive values of gain, the system operates under closed-loop negative feedback and generates interesting eigenvalue trajectories. For example, the solid black lines in the VGMP and VGAP represent the locus of the pole pair that originates on the real axis. The solid gray lines in these plots track the locus of the poles that start as a complex conjugate pair. Notice that when a given pole pair is complex, the two poles have the same

magnitude but are distinguished in angle. Conversely, when poles lie on the real axis, they have a principal angle of either  $-180^\circ$  or  $0^\circ$  corresponding to negative or positive real values, respectively. Furthermore, the VGPs show that the system is stable only for a specific range of  $k$ . The range matches that given in equation (15). Figure 13 is an enlargement of a section of the VGAP highlighting this stable region of the closed-loop system from which the gains may be read directly. The  $90^\circ$  boundary is marked in the figure in accordance with the criterion presented in equation (11).

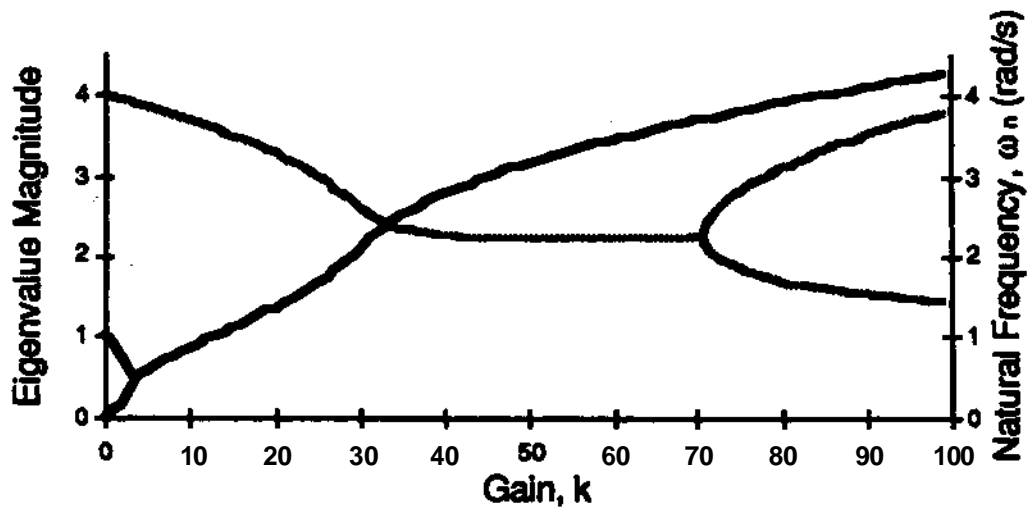


Figure 12a. VGMP for System Given by Equation (14).

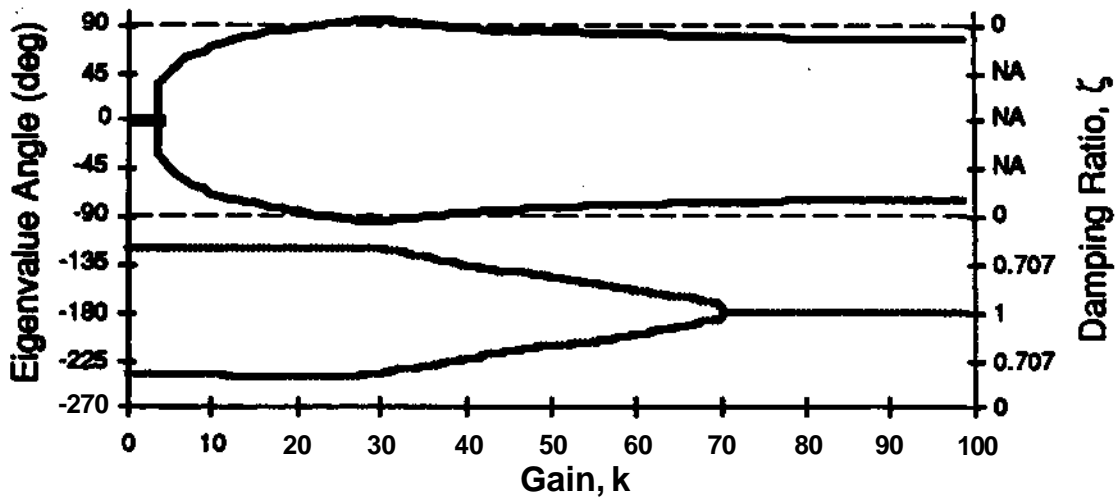


Figure 12b. VGAP for System Given by Equation (14).

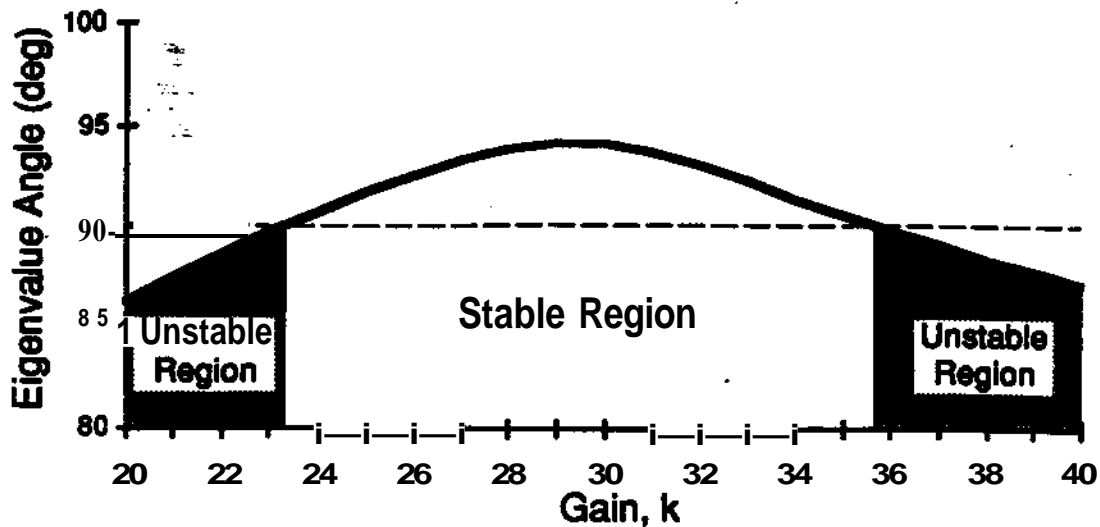


Figure 13. Expanded VGAP for System Given by Equation (14).

The high gain asymptotes of the root locus are found by examining the VGAP for large values of  $k$ . The finite zero at  $s=-1$  is identified by the single pole asymptotically approaching unity magnitude at an angle of  $-180^\circ$ . The remaining three eigenvalues asymptotically approach infinite zeros at angles  $\pm 60^\circ$  and  $-180^\circ$ . For gains higher than those reported in Figure 12a,b, these asymptotes are increasingly prominent

Further inspection of the VGPs provides information about the closed-loop system sensitivity to changes in gain. In the example, the system is highly sensitive to gain variations when  $k$  is small as evidenced by the rapid change in both the angle and magnitude of the system eigenvalues. This behavior is noticeable at  $k \sim 3.1$ , where the angle of the unstable pole pair rises abruptly. Sensitivity information is not readily available from the standard root locus plot (Although unwieldy, some measure of sensitivity can be estimated from the root locus by noting changes in the distances between tick marks of equal increment gain.)

### MIMO Examples

In the MIMO examples presented below, the system is embedded in the closed-loop feedback configuration of Figure 14. The input-output dynamics are now described by a square transfer function matrix,  $G(s)$ , whose elements are transfer functions. For the examples, the controller is  $K(s) = kI$ , implying that each input channel is scaled by the same constant gain  $k$ . The internal structure of  $G(s)$  is given by the state-space equations:

$$\dot{\mathbf{x}}(t) = \mathbf{A}\mathbf{x}(t) + \mathbf{B}\mathbf{u}(t) \quad (16)$$

$$\mathbf{y}(t) = \mathbf{C}\mathbf{x}(t) \quad (17)$$

where  $\mathbf{x}$  is the state vector of length  $n$ ,  $\mathbf{u}$  is the input vector of length  $m$ , and  $\mathbf{y}$  is the output vector of length  $m$ . Matrices  $\mathbf{A}$ ,  $\mathbf{B}$  and  $\mathbf{C}$  are the system matrix, the control influence matrix, and the output matrix, respectively, with appropriate dimensions. The feedback law

$$\mathbf{u}(t) = \mathbf{k}\mathbf{e}(t) \quad (18)$$

is specified where the error vector,  $\mathbf{e}$ , is

$$\mathbf{e}(t) = \mathbf{r}(t) - \mathbf{y}(t) \quad (19)$$

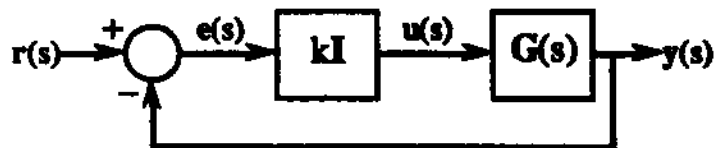


Figure 14. Closed-Loop MIMO Negative Feedback Configuration.

The eigenvalues of the closed-loop system,  $s = X_j$  ( $j=1,2,\dots,n$ ), are the roots of  $\phi_{CL}(s)$ , the closed-loop characteristic polynomial,

$$\phi_{CL}(s) = \phi_{OL}(s) \det[\mathbf{I} + \mathbf{k}\mathbf{G}(s)] \quad (20)$$

where the transfer function matrix  $\mathbf{G}(s)$  is

$$\mathbf{G}(s) = \mathbf{C}[s\mathbf{I} - \mathbf{A}]^{-1}\mathbf{B} \quad (21)$$

and where  $\phi_{OL}(s)$  is the open-loop characteristic polynomial,

$$\phi_{OL}(s) = \det[s\mathbf{I} - \mathbf{A}] \quad (22)$$

By equating the determinant in equation (20) to zero, the MIMO generalization of equation (4) is obtained. The presence of the determinant is the major challenge in generalizing the SISO root locus sketching rules to MIMO systems. The closed-loop system eigenvalues may also be determined from equations (16) - (18) as

$$X_i = \text{eig}[\mathbf{A} - \mathbf{B}(\mathbf{k}\mathbf{I})\mathbf{C}] \quad (23)$$

In the examples, the loci of closed-loop eigenvalues are calculated from equation (23) as  $k$  is monotonically increased from zero.

### Decoupled MIMO Example

This example demonstrates the use of the VGPs for exploring the behavior of a decoupled multivariable system. The state space representation of the system is

$$\dot{\mathbf{x}}(t) = \begin{bmatrix} -1 & 0 \\ 0 & -2 \end{bmatrix} \mathbf{x}(t) + \begin{bmatrix} 1 & 0 \\ 0 & 1 \end{bmatrix} \mathbf{u}(t) \quad (24)$$

$$= \begin{bmatrix} 1 & 0 \\ 0 & 1 \end{bmatrix} \mathbf{x}(t) \quad (25)$$

corresponding to the transfer function matrix

$$\mathbf{G}(s) = \begin{bmatrix} \frac{1}{s+1} & 0 \\ 0 & \frac{1}{s+2} \end{bmatrix} \quad (26)$$

It represents two first order SISO systems with eigenvalues at  $s = \{-1, -2\}$ . Since the system is decoupled, the multivariable root locus may be considered to be the superposition of two SISO root locus plots. That is, the MIMO root locus diagram depicts two eigenvalue trajectories, one beginning at  $s = -1$  and the other beginning at  $s = -2$ . Both trajectories follow a straight line path along an angle of  $-180^\circ$ . Figure 15 presents the root locus for this MIMO decoupled system. Notice that it does not follow the rules of the familiar SISO root locus (e.g., the SISO rule for the portion of the root locus on the real axis is violated), and is not intuitive.

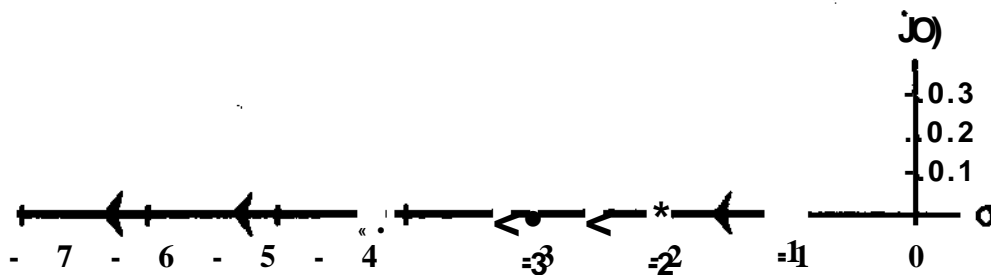


Figure 15. Root Locus for System Given by Equations (24) - (26).

Figure 16 is the VGMP for this decoupled MIMO system. Although not shown, the VGAP indicates that both eigenvalues have angles of  $-180^\circ$ . Thus, the two open-loop eigenvalues are at  $s = \{-1, -2\}$ . Furthermore, as  $k$  increases, both eigenvalues proceed deeper into the left half plane along the  $-a$  axis at the same constant rate. From the VGMP,

there is no ambiguity as to the number or location of the poles. Thus, the VGPs provide significantly more insight into the behavior of the closed-loop system.

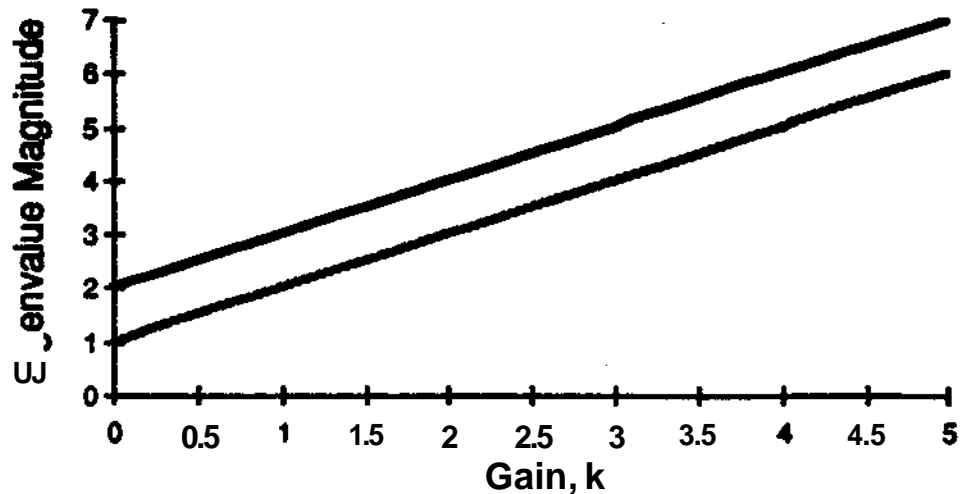


Figure 16. VGMP for System Given by Equations (24) - (26).

### Coupled MIMO Example

This example demonstrates the use of the VGPs for understanding the closed-loop behavior of a coupled multivariable system. Again, the system is assumed to be embedded in the closed-loop configuration of Figure 14. The plant dynamics are now given by the state space model

$$\dot{\mathbf{x}}(t) = \begin{bmatrix} -1 & 0 \\ 0 & -2 \end{bmatrix} \mathbf{x}(t) + \begin{bmatrix} 1 & 1 \\ 3 & 2 \end{bmatrix} \mathbf{u}(t) \quad (27)$$

$$\mathbf{y}(t) = \begin{bmatrix} -1 & 1 \\ -3 & 2 \end{bmatrix} \mathbf{x}(t) \quad (28)$$

corresponding to the transfer function matrix

$$\mathbf{G}(s) = \begin{bmatrix} \frac{(s-D)}{(s+1)(s+2)} & \frac{s}{(s+1)(s+2)} \\ \frac{-6}{L(s+1)(s+2)} & \frac{(s-2)}{(s+1)(s+2)} \end{bmatrix} \quad (29)$$

(Equation (29) is used as an example by Postlethwaite and MacFarlane, 1979, and later by Yagle, 1981.) This coupled MIMO system has eigenvalues at  $s = \{-1, -2\}$ . Since the system is coupled, the multivariable root locus is more complicated than superimposed SISO root locus plots. The MIMO root locus diagram shown in Figure 17 depicts two

**eigenvalue trajectories, one beginning at  $s \gg -1$  and the other beginning at  $s \gg -2$ .** As in the decoupled **example**, the eigenvalue at  $s \gg -2$  follows a real axis trajectory along an angle of  $-180^\circ$ . The eigenvalue at  $s = -1$  does not follow the same trajectory. It initially migrates to the right, proceeding to  $s = 1/24 \sim 0.042$ , and then reverses. As  $k$  is increased, the pole moves back to the left of the imaginary axis along a  $-180^\circ$  asymptote\*. For all values of  $k$ , both eigenvalues are purely real. Notice that Figure 17 does not follow the rules of the familiar SISO root locus, and is extremely counter intuitive.

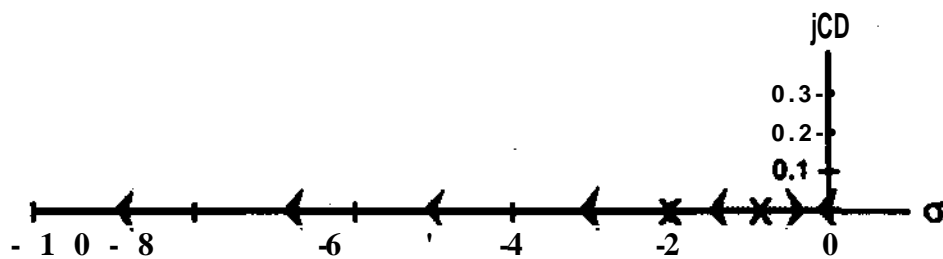


Figure 17. Root Locus for System Given by Equations (27) - (29).

Figure 18a,b presents the VGPs for the coupled MIMO system. Figure 19 is an expanded version of the VGMP that presents the unstable region with higher resolution. It is clear that gain values in the range

$$1 * f c \leq 2 \tag{30}$$

yield an unstable closed-loop system. Figure 19 confirms the maximum magnitude of the eigenvalue at  $0^*$ . An abrupt change in eigenvalue angle occurs when the closed-loop system becomes unstable. This is **expected** since there is a  $180^\circ$  jump in angle as the eigenvalue passes through the origin, highlighting the stable-unstable transition.

The standard root locus plot of this coupled MIMO example is confusing because of the collapse of the Riemann surface into a single complex plane. Since the plot is drawn in two dimensions, branch points may be generated by more than one gain value and, therefore, may not be uniquely presented. The VGPs, however, display eigenvalue magnitude and angle information in an unambiguous and concise manner.

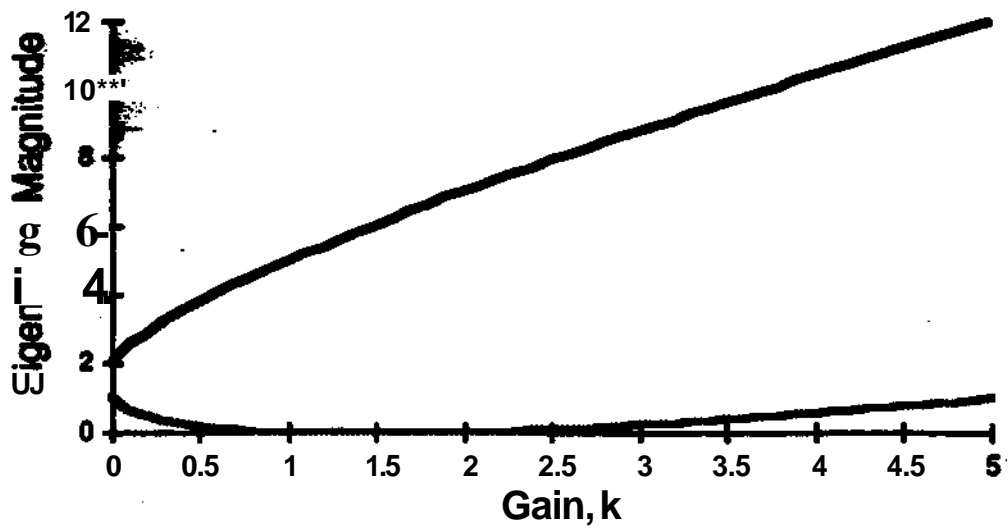


Figure 18a. VGMP for System Given by Equations (27) - (29).

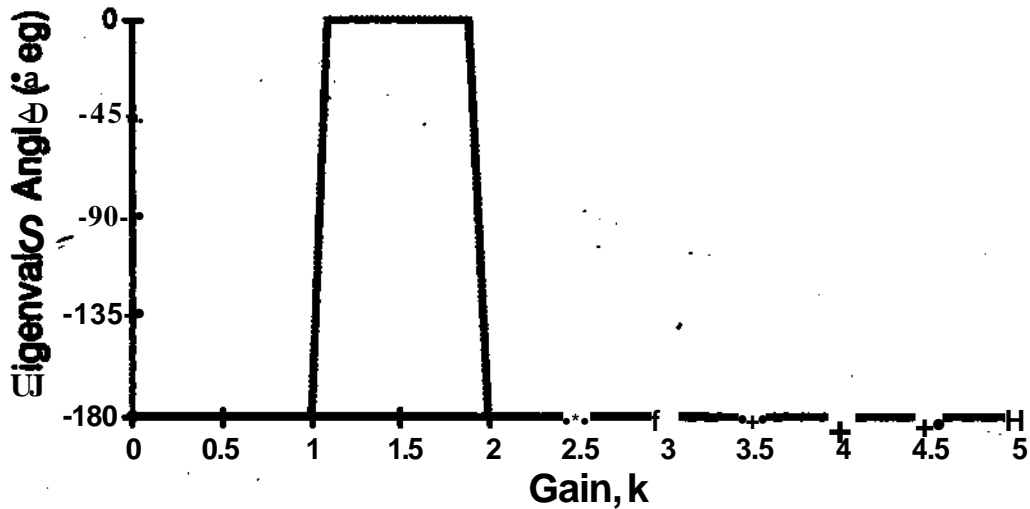


Figure 18b. VGAP for System Given by Equations (27) - (29).

## Conclusions

The Variable Gain Plots developed in this report are a set of illuminating plots that expand and enhance the control engineers' design tool set. Just as Bode plots supplement the information given in the Nyquist diagram, VGPs complement the root locus presentation by recasting it in a new and enlightening manner. By presenting the magnitude and phase in separate graphs, Bode plots simplify the information contained in the Nyquist diagram. As such, the Bode plots add a third "dimension" to the Nyquist

diagram. Analogously, the VGPs are designed to supplement the root locus by adding a third "dimension." In the Bode plots, the common axis linking magnitude and argument is angular frequency; in the VGPs, the common axis bridging magnitude and argument is gain.

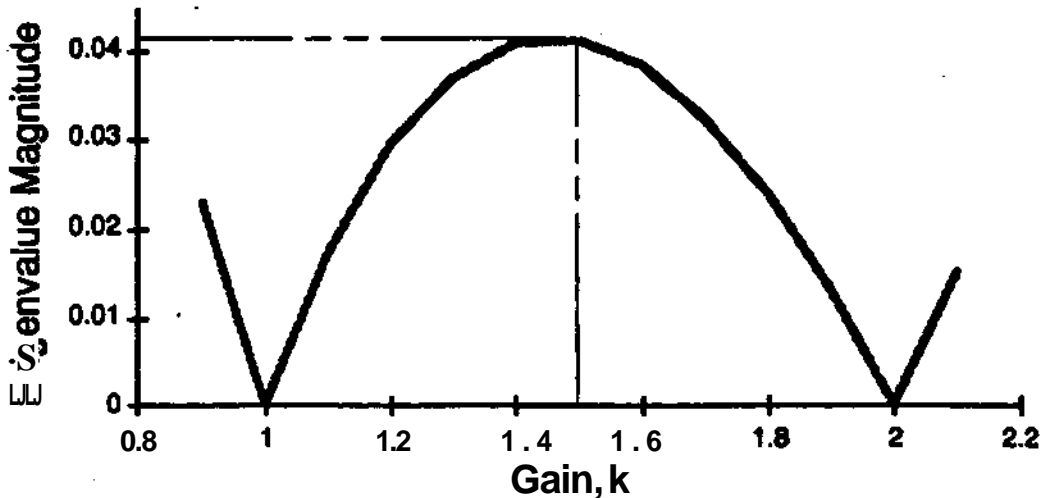


Figure 19. Expanded VGMP for System Given by Equations (27) - (29).

Figure 20 highlights the correspondence of four classical controls graphical tools. As shown, the VGPs fill what may be viewed as a "missing" quadrant of the classical controls tool set. The first row portrays the Nyquist diagram and the Evans root locus spanning a two-dimensional complex plane. The second row shows the Bode plots and VGPs spanning a three-dimensional (real) space. The columns show the variable that is used to increase the dimension, i.e., frequency for Bode plots, gain for VGPs.

The proposed VGPs enhance the root locus by explicitly portraying the relationship between the gain and the location of each eigenvalue whose trajectories are mapped by the root locus. This information is not readily available from the root locus plot. The enhancement enables the control designer to identify, by observation, an eigenvalue location with a specific gain, and hence directly view the influence of the gain on stability as well as on system performance. Furthermore, the VGPs provide a direct measure of eigenvalue gain sensitivity. The change in eigenvalue for a given change in gain is indicated by the slope of the magnitude and angle VGPs. This measure of sensitivity highlights the "cost" of selecting eigenvalue locations corresponding to high gain values.

Many similarities and differences exist between the root locus and the VGPs. For example, both the root locus plot and the VGPs can be drawn for systems with

transportation or dead time. Unlike the root locus plot, the VGPs explicitly highlight open-loop poles near or at transmission zeros. These poles are depicted as horizontal lines indicating constant magnitude and angle for all gains. In the root locus plot pole-zero cancellations are normally camouflaged.

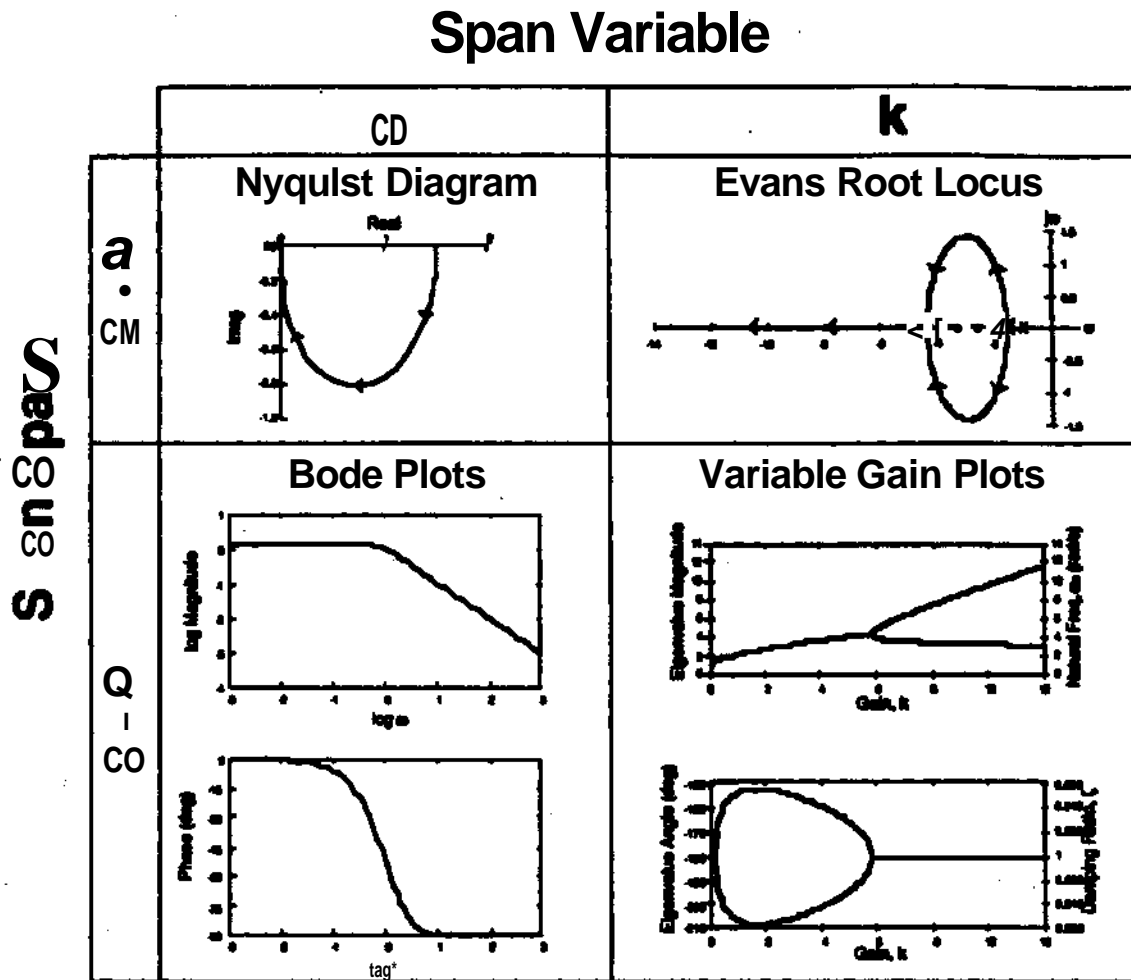


Figure 20. A Unified Control Design Domain.

Further work is necessary to develop intuitive geometric relationships between the Bode plots that present open-loop information and the VGPs that present closed-loop information (for  $k \neq 0$ ). The Nichols chart may provide the appropriate connection. It presents the relationship between the frequency response of the open-loop system and that of the closed-loop system. In so doing, it displays four dimensions of information (*i.e.*, open and closed loop gain and magnitude) in a two-dimensional format where  $\omega$  is the implicit variable. The Nichols chart is a challenging chart to generate and comprehend; however, it does provide a bridge between open-loop and closed-loop systems in the

frequency domain. If the connection between Bode plots and VGPs is made, then some of the more powerful frequency domain synthesis tools may find new applications in control theory.

Future work is also targeted at developing analogous "root locus"\* rules for sketching the VGPs. Although it appears possible to identify these rules, their utility may be limited given the ability for real-time computer implementation\*

Finally, it appears that VGPs offer significant advantages over standard root locus plots for MIMO systems. The major enhancement is the generation of eigenvalue trajectories that are represented as a function of  $k$  (where the compensation has been assumed to be the same static gain applied to all channels). The VGP representation provides a unique description of the eigenvalues. Typical root locus plots do not necessarily generate unique trajectories, as some branches may overlap. This overlap reduces the usefulness of the MIMO root locus.

Although one may suspect that the concepts of this report are "obvious," they do not appear to be mentioned in the literature nor seem to be known to control designers. The VGPs may be viewed as a missing classical controls tool.

In closing, it is not our intent to claim any credit for the incalculable contributions of Nyquist (1932), Bode (1940), and Evans (1948, 1950), but rather to view their contributions in a new light

## References

- Bode, H. W., "Relations Between Attenuation and Phase in Feedback Amplifier Design/" Bell System Technical Journal, Vol. 19, pp 421-454,1940.
- Evans, W. R., "Graphical Analysis of Control Systems/" Transactions of the American Institute of Electrical Engineers, Vol. 67, pp 547-551,1948.
- Evans, W. R., "Control System Synthesis by Root Locus Method," Transactions of the American Institute of Electrical Engineers, Vol. 69, pp 1-4,1950.
- Nyquist, H., "Regeneration Theory," Bell System Technical Journal, Vol. 11, pp 126-147, 1932.
- Ogata, K., Modern Control Engineering, Prentice Hall, Englewood Cliffs, NJ, 1990.

P05lcthw<itc, L aaidMtcFarlane A. O. J., A Compi\* Variable App<sup>TM</sup>... ^ ^ ^ ^  
of Linear Multivariable Feedback Systems, Lecture Notes ,,, Control and Information  
Science. Springer-VerUg, New York, NY, 1979.

Yagle, A ^, BjBejtieiofMultiYariabl6RomTfln : S, M Thesis, Department of Electrical  
Engineering and Computer Science, Massachusetts Institute of Technology,  
Cambridge, MA, 1981.